Journal of Colloid and Interface Science 340 (2009) 153–159

Contents lists available at ScienceDirect

Journal of Colloid and Interface Science

www.elsevier.com/locate/jcis

Macroscopic and spectroscopic characterization of selenate, selenite, and chromate adsorption at the solid–water interface of γ-Al_2O_3

Evert J. Elzinga [a,*], Yuanzhi Tang [b], Jason McDonald [b], Stephanie DeSisto [b], Richard J. Reeder [b]

[a] Department of Earth and Environmental Sciences, Rutgers University, Newark, NJ 07102, USA
[b] Department of Geosciences and Center for Environmental Molecular Science, Stony Brook University, Stony Brook, NY 11794-2100, USA

ARTICLE INFO

Article history:
Received 22 June 2009
Accepted 12 August 2009
Available online 24 August 2009

Keywords:
Selenate
Selenite
Chromate
γ-Al_2O_3
Adsorption
pH
EXAFS

ABSTRACT

The interaction of selenate, selenite, and chromate with the hydrated surface of γ-Al_2O_3 was studied using a combination of macroscopic pH edge data, electrophoretic mobility measurements, and X-ray absorption spectroscopic analyses. The pH edge data show generally increased oxyanion adsorption with decreasing pH, and indicate ionic strength-(in)dependent adsorption of chromate and selenate across the pH range 4–9, and ionic strength-(in)dependent adsorption of selenite in this pH range. The adsorption of chromate peaks at pH 5.0, whereas for selenate and selenite no pH adsorption maxima are observed. Electrophoretic mobility measurements show that all three oxyanions decrease the zeta potential of γ-Al_2O_3 upon adsorption; however, only selenite decreased the pH_{PZC} of the γ-Al_2O_3 sorbent. EXAFS data indicate that selenite ions are coordinated in a bridging bidentate fashion to surface AlO_6 octahedra, whereas no second-neighbor Al scattering was observed for adsorbed selenate ions. Combined, the results presented here show that pH is a major factor in determining the extent of adsorption of selenate, selenite, and chromate on hydrated γ-Al_2O_3. The results point to substantial differences between these anions as to the mode of adsorption at the hydrated γ-Al_2O_3 surface, with selenate adsorbing as nonprotonated outer-sphere complexes, chromate forming a mixture of monoprotonated and nonprotonated outer-sphere adsorption complexes, and selenite coordinating as inner-sphere surface complexes in bridging configuration.

1. Introduction

The mobility and toxicity of contaminants and trace elements in low-temperature geochemical environments is to a large extent controlled by adsorption reactions that partition these elements to the solid phase, rendering them less mobile and bioavailable. Due to the importance of adsorption processes in determining trace element behavior, there have been numerous studies dealing with the interaction of common trace elements and contaminants with mineral surfaces, aided in recent years by the availability of spectroscopic tools that allow for determination of surface interactions at the molecular scale [1,2]. A primary conclusion from these studies is that contaminant retention at mineral surfaces rarely involves a single mechanism but typically occurs through a number of different sorption processes that vary in importance as a function of system parameters such as pH, ionic strength and reaction time (e.g., [3–8]). This mechanistic variation even in relatively simple model systems necessitates studies where environmentally relevant parameters are varied over ranges representative of values found in environmental settings in order to obtain a comprehensive understanding of environmental contaminant behavior.

Aluminum oxides are among the most abundant and reactive minerals found in soils and sediments, and may control or influence the environmental behavior of numerous trace elements and contaminants, including divalent metals such as Pb^{2+}, Zn^{2+} and Ni^{2+} [9–11], actinides [12–15], organic ions [16–18], and oxyanions such as arsenate, selenate and sulfate [8,16,19–23]. The high reactivity of these minerals is due to a combination of small particle size leading to large specific surface area and high density of reactive surface functional groups capable of protonation/deprotonation as well as of complexation reactions with a variety of cations and anions [24]. The high pH_{PZC} of aluminum oxides, typically near pH 9 [25], results in a net positive charge on the surfaces of these minerals under most environmental conditions, which may facilitate adsorption of anions as outer-sphere complexes held by electrostatic interactions, as has been suggested for, e.g., selenate and sulfate anions adsorbed to γ-Al_2O_3 [20]. Anions can also coordinate to the surface through ligand exchange reactions resulting in the formation of inner-sphere adsorption complexes, as has been observed for, e.g., arsenate adsorption on γ-Al_2O_3 and selenate adsorption on corundum [8,19,21]. Inner-sphere complexation as well as induced surface precipitation and polymerization have been reported in the interaction of metals with alumina surfaces [9–11,26–29]. Operative retention mechanisms depend on the specific mineral phase and trace ele-

* Corresponding author.
E-mail address: elzinga@andromeda.rutgers.edu (E.J. Elzinga).

0021-9797/$ - see front matter © 2009 Elsevier Inc. All rights reserved.
doi:10.1016/j.jcis.2009.08.033

ments or contaminant considered, as well as on the reaction conditions applied.

In this study, we investigated the interaction of selenate, selenite, and chromate with the surface of γ-Al_2O_3 as a function of pH and ionic strength using macroscopic methods in combination with X-ray absorption spectroscopy (XAS). Selenate (SeO_4^{2-}) and selenite (SeO_3^{2-}) are the oxyanions of the 6+ and 4+ valence ions of selenium, respectively, whereas chromate (CrO_4^{2-}) is the oxyanion of hexavalent Cr. Previous studies on the adsorption of these oxyanions have shown that selenate and chromate generally adsorb weakly at mineral surfaces through electrostatic interactions, whereas selenite is much more reactive and forms inner-sphere complexes on the surfaces of a variety of minerals [22,23,30–36]. This general difference in reactivity implies that selenate and chromate are more mobile and soluble than selenite in aqueous environmental settings.

We are not aware of spectroscopic studies on the interaction of chromate with Al(III)-(hydr)oxide surfaces; for selenate and selenite, however, spectroscopic studies addressing the interaction of these ions with the surfaces of aluminum oxides and hydroxides have been reported. Papelis et al. [26] used extended X-ray absorption fine structure spectroscopy (EXAFS) to characterize the surface complexes of selenite on corundum and gibbsite. On both Al substrates, selenite was found to form mononuclear complexes with three O atoms in the first coordination shell; although no Al scattering could be positively identified in the EXAFS data of adsorbed selenite, the independence of selenite adsorption on ionic strength suggested inner-sphere complexation of selenite on these sorbents. Boyle-Wight et al. [27,28] used EXAFS to study selenate and selenite speciation in γ-Al_2O_3 suspensions in the presence and absence of Co(II). These authors found that selenate did not affect Co(II) sorption by γ-Al_2O_3, whereas selenite enhanced Co(II) sorption due to formation of ternary Co(II)–selenite complexes and/or the precipitation of selenite/Co(II) phases; the coordination of selenate and selenite to the γ-Al_2O_3 surface in binary selenite– or selenate–γ-Al_2O_3 systems was not addressed in this study. Wijnja and Schulthess [20] used ATR-FTIR and Raman spectroscopy to study the interaction of selenate and sulfate with γ-Al_2O_3 and concluded that these oxyanions predominantly adsorb as outer-sphere complexes in the pH range 4–7, with a small fraction of inner-sphere complexation occurring at pH < 6. Peak and co-workers [22,23] used EXAFS to address the adsorption of selenate and selenite to a variety of Al substrates and argued for structure based reactivity of Al oxides, with hydrous Al oxides forming outer-sphere complexes with selenate (and its chemical analogue sulfate), and inner-sphere monodentate complexes form between selenate and corundum. For selenite, a mixture of inner- and outer-sphere complexes at the surface of hydrous Al oxide was observed [22,23].

In the current study, we used a combination of macroscopic pH edge data, electrophoretic mobility measurements, and X-ray absorption spectroscopic analyses to provide further insights into the interaction of selenate, selenite, and chromate with the surface of hydrated γ-Al_2O_3. The results indicate significant differences in the mode of adsorption of these ions at the γ-Al_2O_3 surface, and indicate that pH dictates the uptake of these ions by γ-Al_2O_3 due to its effect on surface charge, the concentration of OH^- ions that compete with oxyanions for adsorption at the surface, and the oxyanion protonation state.

2. Materials and methods

2.1. Materials

The alumina sorbent used in the studies described here was γ-Al_2O_3 obtained from Degussa, a material that has been used as a sorbent in many other studies (e.g., [8,9,20]). The manufacturer reports a purity of >99.6%, an average particle size of 13 nm, and a BET surface area of 100 ± 15 m^2 g^{-1} for this material. Electrophoretic measurements (described below) indicated a point of zero charge a approximately pH 9.2. Adsorption experiments described were performed using γ-Al_2O_3 suspensions that had been aged for approximately 15 h. Hydration at pH > 5 slowly transforms γ-Al_2O_3 to the gibbsite and bayerite polymorphs of $Al(OH)_3$ [13,37,38]. The short hydration period employed likely mostly lead to transformation of the surface region of γ-Al_2O_3 particles [37]. All chemicals used were ACS reagent grade or better.

2.2. pH edge experiments

Sample pH values in the pH edge experiments ranged between pH 4 and 9. Each set of pH edge experiments was run in 0.01 M and 0.15 M NaCl background electrolytes to investigate the effect of ionic strength on selenite, selenate, and chromate uptake by γ-Al_2O_3. To exclude CO_2, the experiments were performed in a glove box with an N_2 atmosphere, using boiled DDI-H_2O for sample and reagent preparation.

Samples for each pH edge experiment were prepared from a 250-ml suspension of 10 g L^{-1} γ-Al_2O_3 in either 0.01 M or 0.15 M NaCl, which had been aged for at least 15 h. The suspension pH was raised to 9.5 using a small aliquot of 0.1 M NaOH, and an appropriate amount of a 0.1 M K_2CrO_4, Na_2SeO_4, or Na_2SeO_3 stock solution was added to achieve a concentration of 1 mM of the anion of interest. Two 10-ml duplicate samples were then transferred to 30 mL centrifuge tubes, which were sealed, placed in zip lock bags inside the glove box, and then transferred to a reciprocal shaker for equilibration outside the glove box. The remainder of the suspension was titrated to lower pH values by stepwise addition of 0.1 M HCl. After each pH decrement, two 10-ml subsamples were transferred to the reciprocal shaker as described above. The samples were reacted for 24 h, measured for pH in the glove box, and centrifuged at 15,550 *g* for 10 min. The supernatants were passed through 0.22-μm filters, acidified, and analyzed for dissolved selenium or chromium concentration using direct current plasma (DCP) spectrometry. Oxyanion adsorption was calculated from the difference between the initial and final solution concentrations.

2.3. Electrophoretic mobility measurements

The samples for the electrophoretic mobility measurements had a γ-Al_2O_3 suspension density of 0.1 g L^{-1} in a 0.01 M NaCl background electrolyte with pH values in the range of 4–9.5. Sample preparation was similar to that for the pH edge experiments described above, involving stepwise titration and subsampling of an aged aqueous γ-Al_2O_3 suspension. To assess the effect of oxyanion sorption on the electrophoretic mobility of the γ-Al_2O_3 particles, samples were prepared both in the presence and in the absence of SeO_4^{2-}, SeO_3^{2-}, or CrO_4^{2-} across the pH range 4.0–9.5; the oxyanion-spiked suspensions had a concentration of SeO_4^{2-}, SeO_3^{2-} or CrO_4^{2-} of 1 mM. The suspensions were allowed to equilibrate for 24 h and were then analyzed for pH and transferred to cuvets for analysis of electrophoretic mobility. A Brookhaven ZetaPlus analyzer (Brookhaven Instruments Coporation, Holtsville, NY) was used for the electrophoretic mobility measurements. Five measurements per sample were taken and averaged.

In preliminary experiments, samples for the electrophoretic mobility measurements were prepared both inside and outside the glove box to check for possible effects of CO_2 and O_2 on the results. No systematic differences between the datasets were observed, and subsequent sample preparation for the mobility measurements was therefore performed outside the glove box;

the electrophoretic mobility results presented below were obtained for samples prepared under ambient atmospheric conditions.

2.4. EXAFS spectroscopy

EXAFS samples were prepared in a N_2-filled glove box under experimental conditions identical to those for the samples in the pH edge experiments described above, except for total volume, which was increased to 30 mL to obtain sufficient γ-Al_2O_3 material for EXAFS analysis. Following reaction for 24 h, the suspension pH was measured, and the γ-Al_2O_3 sorbent of each sample was collected by centrifugation for 10 min at 15,550 *g* and loaded as a wet paste in a Lucite sample holder, which was then sealed with Kapton tape. The samples were stored in Ziplock bags inside the glove box before being transported to the synchrotron facility for EXAFS analysis. Spectroscopic measurements were performed within 3 days following sample preparation.

EXAFS spectra of the Se-reacted γ-Al_2O_3 were recorded at beamline X18B of the National Synchrotron Light Source at Brookhaven National Laboratory. The storage ring operated at 2.84 GeV with a maximum current of 280 mA. A channel-cut Si(1 1 1) crystal was used in the monochromator, with detuning of 25% for harmonic rejection. Multiple scans (3–10, depending on the sample) of the γ-Al_2O_3 adsorption samples were collected at the Se *K*-edge (12,658 eV) at room temperature, using a solid state PIPS detector for fluorescence detection. Individual scans were carefully checked for any changes during sample runs, which were not observed. Scans were then calibrated and averaged prior to fitting. Further data reduction and fitting were performed with the WinXAS2000 software package [39] using standard procedures.

Attempts were also made to collect EXAFS data of chromate-reacted γ-Al_2O_3 samples at the Cr *K*-edge (5989 eV). The XAS data of these CrO_4^{2-} samples, however, showed evidence for progressive beam-induced reduction of Cr(VI) to Cr(III) during successive scans. Sample freezing and analysis at 77 K decreased but did not prevent beam damage; time limitations prevented us from exploring additional strategies to prevent beam-induced Cr reduction in these samples, and ultimately we were not successful in collecting reliable XAS data for the CrO_4^{2-} samples. Characterization of CrO_4^{2-} interactions with γ-Al_2O_3 provided here is therefore limited to the uptake trends seen in the macroscopic data, which provide indirect indications on mechanistic processes at the molecular scale.

Theoretical backscattering paths were calculated with FEFF7 [40]. Fitting was done in *R* space out to approximately 4 Å without constraints on the fitting parameters (coordination number, radial distance, and Debye–Waller factor) of individual shells. The amplitude reduction factor was set at 1.0, and a single global E_0 value was allowed to float during fitting. The number of parameters allowed to vary never exceeded the Nyquist limit. Error estimates are ±0.02 Å for the radial distance (*R*) values of the first shells, and ±0.05 Å for higher shells. For the coordination number (CN), which is correlated with the Debye–Waller factor, the error is estimated at ±15% for the first O shell, and >25% for the further shells.

3. Results

3.1. pH edges

The pH edges of SeO_4^{2-}, SeO_3^{2-} and CrO_4^{2-} uptake on γ-Al_2O_3 are presented in Fig. 1. The general trends in the pH dependence of uptake of the three oxyanions are similar in that sorption decreases with increasing pH; however, the uptake patterns differ in detail, with selenite reaching 90% uptake at pH 7 and nearly complete uptake at pH < 6 (Fig. 1A), selenate showing a monotonic increase in adsorption with decreasing pH across the pH range (Fig. 1B), and chromate adsorption peaking at pH 5 (Fig. 1C). Striking differences are seen with respect to the effect of ionic strength on oxyanion uptake, with CrO_4^{2-} and SeO_4^{2-} showing substantial decreases in sorption with increasing ionic strength (Fig. 1C and B), whereas SeO_3^{2-} uptake is essentially independent of ionic strength under the conditions investigated here (Fig. 1A).

The general increase in sorption with decreasing pH for these oxyanions can be attributed to reduced competition with OH^- for coordination at surface sites and/or an increase in positive surface charge due to increased protonation of amphoteric surface sites

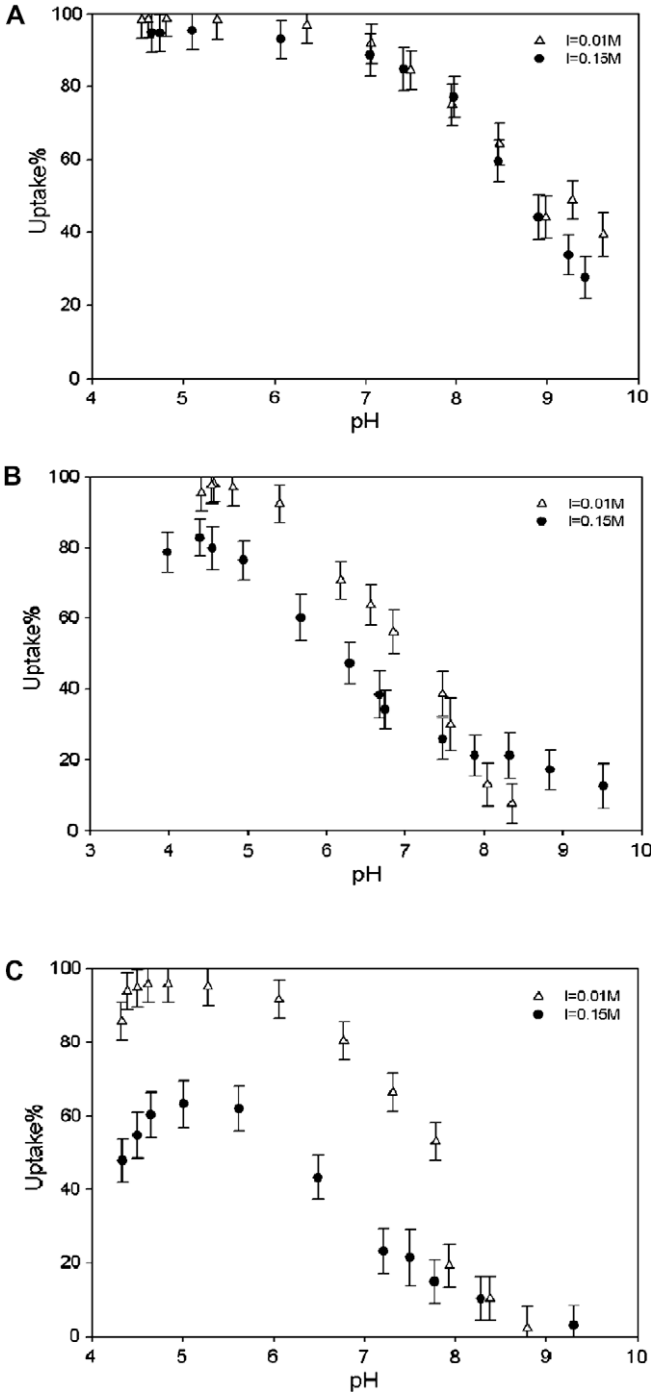

Fig. 1. pH edges of the adsorption of selenite (A), selenate (B), and chromate (C) onto γ-Al_2O_3 in 0.15 M and 0.01 M NaCl background electrolytes.

when pH is lowered. Sorption maxima in pH edges of oxyanions such as seen here for chromate are typically attributed to changes in solution speciation due to protonation/deprotonation reactions changing sorbate reactivity towards adsorption [24]. The effect of ionic strength as seen here for chromate and selenate uptake is a classical macroscopic indication of the occurrence of outer-sphere (electrostatic) adsorption processes, as first suggested by Hayes and Leckie [41], and applied in many studies since (e.g., [3,4,8,26]). The data presented in Fig. 1 therefore suggest that both selenate and chromate interact electrostatically with the γ-Al_2O_3 surface, whereas selenite (SeO_3^{2-}) forms inner-sphere complexes. In the absence of spectroscopic data or data from additional techniques characterizing oxyanion adsorption, statements on molecular level processes explaining the observed macroscopic trends remain speculative. We will use the results of the electrophoretic mobility measurements and EXAFS spectroscopic analyses discussed below to further constrain the mechanistic underpinnings of the observed pH trends and ionic strength effects.

3.2. Electrophoretic mobility measurements

The electrophoretic measurement results are presented in Fig. 2, where the effect of pH and oxyanion sorption on the electrophoretic mobility of the γ-Al_2O_3 particles are evaluated by comparing the pH dependent mobility measurements of clean (i.e., unreacted) and oxyanion-sorbed γ-Al_2O_3. For the unreacted material, the pH of point of zero charge (pH_{PZC}) is found at pH ~ 9.2, which is consistent with results from previous studies characterizing the surface charge of this sorbent [25]. At pH values below the pH_{PZC}, the surface charge of the unreacted γ-Al_2O_3 increases to more positive values when pH is lowered from 9.2 to ~7 but then stabilizes at lower pH values, indicating that protonation of amphoteric surface sites is complete. At pH values above the pH_{PZC}, the alumina sorbent has a negative surface charge, which increases when pH is increased from the pH_{PZC} = 9.2 to pH 10, the highest pH value used in this study.

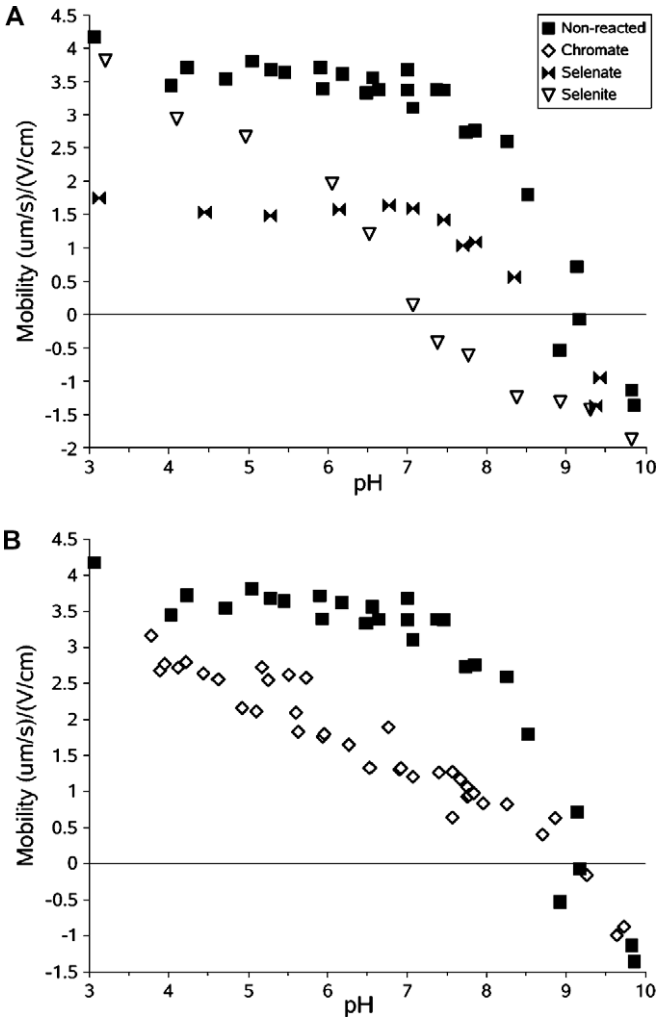

Fig. 2. Electrophoretic mobility data of nonreacted γ-Al_2O_3 compared to γ-Al_2O_3 reacted with 1 mM selenate or selenite (A) and chromate (B). The γ-Al_2O_3 suspensions had a particle loading of 0.1 g L^{-1} and a 0.01 M NaCl background.

Comparison of the electrophoretic data of oxyanion-reacted γ-Al_2O_3 and clean (unreacted) γ-Al_2O_3 indicates that the reaction of selenite with the alumina material lowers the pH_{PZC} of γ-Al_2O_3, whereas the adsorption of selenate and chromate does not change the pH_{PZC} (Fig. 2). Lowering of the pH_{PZC} upon reaction is a macroscopic indication of inner-sphere anion complexation [42], as it indicates the presence of additional negative charge within the shear plane near the alumina surface that requires additional site protonation (i.e., a lower pH) to achieve surface charge neutrality. The combination of the electrophoretic mobility data (Fig. 2) and the selenite pH edge data of Fig. 1, which indicate no ionic strength effect on selenite adsorption by γ-Al_2O_3, and thus strongly suggests predominantly inner-sphere complexation of selenite ions at the γ-Al_2O_3 surface. EXAFS data of adsorbed selenite species will be presented in the next section to further characterize the interaction of selenite with the γ-Al_2O_3 surface.

In contrast to selenite, reaction with selenate and chromate oxyanions does not shift the pH_{PZC} of γ-Al_2O_3 (Fig. 2). This may indicate: (i) the formation of outer-sphere selenate and chromate complexes that do not change surface charge; (ii) the absence of appreciable adsorption of selenate and chromate at the relative high pH_{PZC} (near 9) of the alumina material; and/or (iii) adsorption of neutral (protonated) selenate and chromate species at the γ-Al_2O_3 surface. Factors (i) and (ii) are supported by the chromate and selenate pH edges (Fig. 1A and B), showing ionic strength dependence of selenate and chromate adsorption by γ-Al_2O_3 suggestive of outer-sphere complexation, and limited (although not fully inhibited) adsorption of chromate and selenate near the pH_{PZC}. The presence of neutral species adsorbing seems unlikely, as the zeta potential is reduced (i.e., less positive) in the chromate and selenate containing systems relative to the unreacted γ-Al_2O_3 in the pH range 4–9, indicating that adsorption complexes of selenate and chromate carry a negative charge that lowers the positive charge of the near-surface region bounded by the shear plane. Further discussion on the selenate and chromate adsorption complexes is provided below.

3.3. EXAFS data

The EXAFS data of the selenate and selenite adsorption complexes forming in the pH range 4–8.5 are shown in Fig. 3, with Fig. 3A and B showing the raw and fitted k^3-weighted χ functions, respectively, and Fig. 3C and D showing the corresponding Fourier transforms of the raw k^3-weighted χ data. For reference, Fig. 3 also presents the EXAFS data of aqueous selenate and selenite oxyanions in addition to the sorption samples. The fitting results are summarized in Table 1.

In the case of selenate, the EXAFS data of the adsorption complexes are essentially identical to the data of the aqueous selenate reference (Fig. 3A and C; Table 1). The data are all fitted with approximately four O atoms at a distance of 1.65 Å (Table 1), consistent with a tetrahedral arrangement of O atoms around the Se(VI) central atom. No significant distortion is observed in

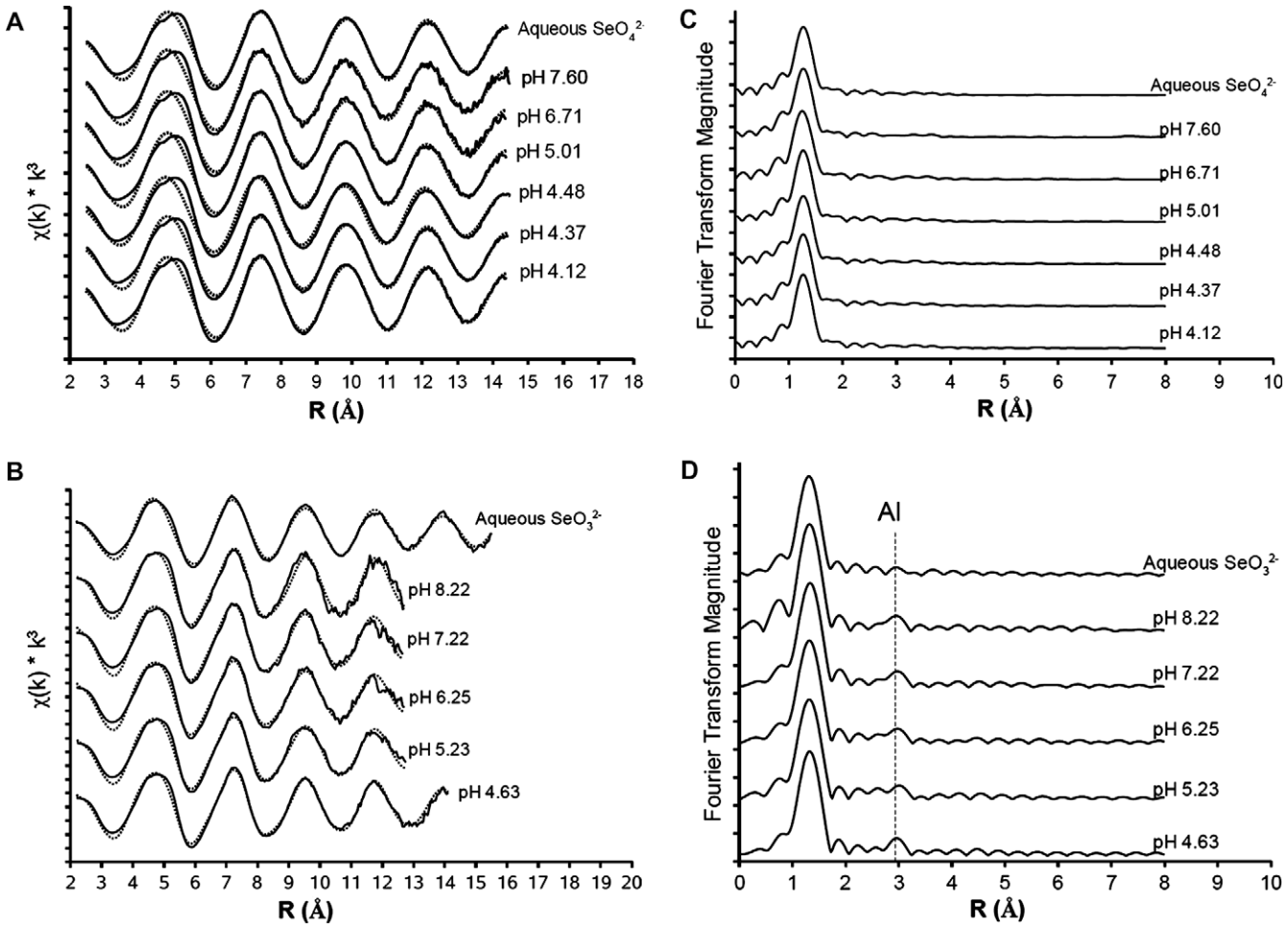

Fig. 3. Raw (solid lines) and fitted (dotted lines) χ spectra of selenate (A) and selenite (B) adsorption complexes and aqueous references; the corresponding Fourier transforms are shown in (C) for selenate and in (D) for selenite.

Table 1
EXAFS fitting results for the selenate (SeVI) and selenite (Se(IV)) adsorption samples and aqueous standards.

Sample	pH	Shell	CN[a]	R(Å)[b]	σ^2 (Å^2)[c]
Se(VI) aqueous standard		Se–O	3.6	1.65	0.0012
Se(VI)-γ-Al_2O_3	7.60	Se–O	4.1	1.65	0.0019
Se(VI)-γ-Al_2O_3	6.71	Se–O	4.1	1.65	0.0016
Se(VI)-γ-Al_2O_3	5.01	Se–O	4.0	1.65	0.0015
Se(VI)-γ-Al_2O_3	4.48	Se–O	3.9	1.65	0.0017
Se(VI)-γ-Al_2O_3	4.37	Se–O	4.0	1.65	0.0014
Se(VI)-γ-Al_2O_3	4.12	Se–O	4.0	1.65	0.0013
Se(IV) aqueous standard		Se–O	2.6	1.70	0.0017
Se(IV)-γ-Al_2O_3	8.22	Se–O	2.9	1.69	0.0015
		Se–Al	1.6	3.20	0.0065
Se(IV)-γ-Al_2O_3	7.22	Se–O	2.9	1.70	0.0020
		Se–Al	1.5	3.22	0.0072
Se(IV)-γ-Al_2O_3	6.25	Se–O	3.1	1.70	0.0026
		Se–Al	1.6	3.21	0.0095
Se(IV)-γ-Al_2O_3	5.23	Se–O	3.0	1.70	0.0023
		Se–Al	1.6	3.20	0.0094
Se(IV)-γ-Al_2O_3	4.63	Se–O	2.9	1.70	0.0019
		Se–Al	1.4	3.22	0.0059

[a] Coordination number.
[b] Radial distance.
[c] Debye–Waller factor.

the first-shell of O atoms of adsorbed selenate as compared to dissolved selenate, as indicated by the similar Debye–Waller factors and coordination numbers of first-shell O fitted for these samples (Table 1), and there is no evidence of second-shell Al scattering in the selenate adsorption samples (Fig. 3A and C). The EXAFS data therefore point to the formation of outer-sphere selenate adsorption complexes electrostatically held by the γ-Al_2O_3 surface. This is consistent with the dependence of selenate adsorption on ionic strength shown in Fig. 1 and the electrophoretic mobility measurements of selenate-reacted alumina shown in Fig. 2.

The EXAFS data of selenite adsorption complexes forming at the γ-Al_2O_3 surface are presented in Fig. 3B. The Fourier transforms and the data fitting results indicate that the EXAFS spectra of both the sorption samples and the aqueous standard are dominated by first-shell O scattering from $R = 1.70$ Å, consistent with a trigonal pyramidal first-shell O configuration. The Fourier transforms of the sorption samples show a second shell at $R \sim 3.0$ Å (uncorrected for phase shift) that is absent in the Fourier transform of the aqueous standard and could be successfully fitted with Al scattering from approximately 3.20 Å (Table 1). The presence of second-shell Al scatterers in the Se(IV)–γ-Al_2O_3 sorption samples indicates the formation of inner-sphere Se(IV) surface complexes that are directly coordinated to surface Al(III) atoms via O-ligands. This is consistent with the macroscopic data showing ionic strength-independent adsorption of Se(IV) across the pH range studied (Fig. 1) and a shift towards lower pH_{PZC} for Se(IV)-reacted alumina as compared to unreacted γ-Al_2O_3 (Fig. 2).

4. Discussion

The macroscopic and spectroscopic results presented here indicate that retention of chromate and selenate at the γ-Al_2O_3 surface following uptake from aqueous solution occurs predominantly by electrostatic interactions, whereas selenite is adsorbed as an inner-sphere complex. The results found here for γ-Al_2O_3 are broadly consistent with studies investigating the reaction of these ions with other mineral surfaces, which generally report relatively weak outer-sphere interactions for selenate and chromate, but indicate inner-sphere coordination of Se(IV) [20,22,23,30–32,43,44]. The weak particle reactivity of chromate and selenate with common minerals, including Al(III) oxides and hydroxides, raises concerns as to the mobility of these oxyanions in environmental settings.

The EXAFS data of the inner-sphere surface complexes of Se(IV) indicate a Se–Al distance of 3.20 Å (Table 1), which can be used to constrain the mode of coordination of Se(IV) to the γ-Al_2O_3 surface based on simple geometric considerations. Assuming a Al–O distances of 1.85–1.97 Å and O–O separations in the range 2.52–2.86 Å for AlO_6 octahedra [45], and accounting for the Se–O distances of 1.70 Å observed for the selenite surface complexes (Table 1), the observed Se–Al distance of 3.2 Å indicates bidentate bridging coordination to surface AlO_6 groups. The same bridging coordination was found for inner-sphere complexes of Se(IV) adsorbed at the surface of hydrous amorphous alumina [22].

Although both chromate and selenate appear to sorb as outer-sphere complexes at the γ-Al_2O_3 surface, the results from the macroscopic pH edge data indicate a difference in the pH dependence of retention of these oxyanions, with selenate sorption increasing monotonically with decreasing pH across the pH range, while chromate sorption reaches a maximum near pH 5.0, and decreases at both higher and lower pH values (Fig. 2). This difference in macroscopic uptake behavior likely reflects molecular level differences in the adsorption of chromate and selenate. In the paragraphs below, we argue that a difference in pH-dependent protonation of these anions causes these different macroscopic trends.

The results of the electrophoretic mobility measurements show that selenate-reacted γ-Al_2O_3 has a pH_{PZC} similar to unreacted γ-Al_2O_3; however, the overall positive surface charge at pH values below the pH_{PZC} is smaller for the SeO_4^{2-}-reacted alumina than for the unreacted material across the entire pH range (Fig. 2). The positive charge of the unreacted γ-Al_2O_3 increases as the pH is lowered from the pH_{PZC} (9.1) to 7, indicating that protonation of surface functional groups occurs primarily in the pH range 7–9.1 and is complete at pH < 7. The surface charge of the SeO_4^{2-}-reacted γ-Al_2O_3 follows the same trend with pH as the unreacted γ-Al_2O_3, but at lower overall (positive) surface charge (Fig. 2). The lower surface charge of the SeO_4^{2-}-reacted alumina as compared to "clean" alumina indicates that adsorbed SeO_4^{2-} contributes (negative) charge to the surface layer bounded by the shear plane. Although the dimensions of the shear plane are not necessarily known, the shear plane is generally assumed to be well within the electrical double layer near the surface [46]. Therefore, the lower zeta potential values observed in the presence of adsorbed SeO_4^{2-} at pH_{PZC} indicate a close association of SeO_4^{2-} anions with the surface, although the occurrence of significant inner-sphere complexation can be ruled out based on the EXAFS data results. The proposed electrostatic nature of the interaction of SeO_4^{2-} with the γ-Al_2O_3 surface is supported by the identical trends in surface charge development as a function of pH (although at different overall values) for the SeO_4^{2-}- and unreacted γ-Al_2O_3 systems (Fig. 2), indicating that adsorption of (zeta-potential-altering) selenate anions at the surface is directly related to the magnitude of the positive surface charge. A mechanism that may account for the combined macroscopic and spectroscopic observations of selenate adsorption on γ-Al_2O_3 would be H-bonding between positively charged surface functional groups and negatively charged selenate ions, as this type of interaction involves electrostatic attraction but requires close proximity (a single water layer) between adsorbate and adsorbent.

Fig. 1B shows increased SeO_4^{2-} sorption as pH is lowered below pH 7, whereas the zeta potential measurements presented in Fig. 2 suggest that SeO_4^{2-} uptake is complete at pH 7 and does not increase further at lower pH values. It is likely that the difference in sorbate:sorbent ratio (i.e., selenate:γ-Al_2O_3) between these experiments plays a role in these different trends: the 50-fold higher selenate:alumina ratio used for the zeta potential measurements as compared to the pH edge experiments may have saturated the sites available for SeO_4^{2-} uptake at pH < 7, whereas for the pH edge experiments competition with OH^- for coordination at surface sites may have affected SeO_4^{2-} sorption at pH < 7 even as the surface charge remained constant.

For chromate, adsorption at the γ-Al_2O_3 surface reaches a maximum at pH 5 (Fig. 1C), and the electrophoretic mobility measurements show that the zeta potential and electrophoretic mobility of CrO_4^{2-}-reacted γ-Al_2O_3 steadily approach the values of clean γ-Al_2O_3 as pH is lowered in the range below the pH_{PZC} (Fig. 2B). The presence of adsorption maxima in the pH edges of oxyanions typically occur near a pK_a value and are commonly attributed to protonation/deprotonation reactions in the aqueous phase altering the reactivity of the adsorbate towards the surface [21]. The pK_a of the reaction $HCrO_4^- \iff CrO_4^{2-} + H^+$ is 6.5 [47], approximately 1.5 pH units above the pH where maximum chromate adsorption is observed in the current results (pH ~ 5.0; Fig. 1C). Calculations of the aqueous speciation of chromate in 0.01 M NaCl using vminteq (Version 2.61) in combination with the MINTEQA2 database indicate CrO_4^{2-} and $HCrO_4^-$ as the main solution species (accounting for >90% of dissolved Cr), and show that the contribution of bichromate $HCrO_4^-$ to total dissolved Cr increases from 41% at pH 6.5 to 89% at pH 5.0. We conclude that the decreased sorption at pH < 5 is due to the increased importance of $HCrO_4^-$ in solution which has an apparently lower affinity for the γ-Al_2O_3 surface than CrO_4^{2-}. Since the interaction of chromate with the γ-Al_2O_3 surface is electrostatic in nature, the lower affinity of $HCrO_4^-$ relative to CrO_4^{2-} is readily explained by the lower charge of $HCrO_4^-$ making interaction less favorable. A build up of adsorbed $HCrO_4^-$ species at the γ-Al_2O_3 surface can explain the electrophoretic mobility data, which show that the zeta potential of chromate reacted γ-Al_2O_3 shifts toward the zeta potential of clean γ-Al_2O_3 as pH is lowered below the pH_{PZC} (Fig. 3). The weaker electrostatic interaction of $HCrO_4^-$ with the alumina surface than for CrO_4^{2-} is likely to result in a longer distance between the surface and adsorbed $HCrO_4^-$ as compared to CrO_4^{2-}, leading to a reduction in (negative) charge being introduced to the near-surface layer bounded by the shear plane in the case of $HCrO_4^-$ adsorption as compared to CrO_4^{2-} adsorption. This is reflected in the electrophoretic mobility data by the decrease in the difference of the surface charge of clean and chromate reacted γ-Al_2O_3 as pH is lowered in the pH range 5–8 (Fig. 2), despite an overall increase in chromate sorption with decreasing pH in this pH range (Fig. 1). At pH < 5, overall sorption decreases and $HCrO_4^-$ concentrations increase further, thus enhancing the similarity in surface charge of unreacted and chromate-reacted γ-Al_2O_3 material (Fig. 2).

The data presented here for selenate and selenite interactions with γ-Al_2O_3 are consistent with previous studies dealing with the interaction of these oxyanions with alumina surfaces. Wijnja and Schulthess [20] studied the interaction of selenate and sulfate with γ-Al_2O_3 using *in situ* ATR-FTIR and Raman spectroscopy over

the pH range 4–7 and concluded that these oxyanions form predominantly outer-sphere complexes across the pH range, with a small fraction of inner-sphere complexation occurring at pH < 6. This is consistent with our findings, except that there is no evidence in our data for the formation of inner-sphere complexation at pH < 6, which may reflect the fraction of any selenate inner-sphere complexes present being below the detection limit of our techniques. The main difference in the EXAFS data of inner- and outer-sphere selenate complexes would be second-shell Al scattering for inner-sphere complexes that would be absent for outer-sphere SeO_4 complexes, similar to the difference in second-shell Fe scattering that has been observed for inner- and outer-sphere complexes of selenate at the surface of Fe(III)-oxides [32]. The low sensitivity of EXAFS for detection of inner-sphere selenate complexes in our samples is likely due to low abundance of any inner-sphere complexes in combination with the weak nature of Al scattering.

Peak [22] studied selenate and selenite adsorption onto hydrous aluminum oxide (HAO) and corundum using EXAFS and concluded that selenate primarily forms outer-sphere complexes on HAO over the pH range 3.5–6.0, but formed monodentate inner-sphere complexes on corundum. For selenite, Peak [22] proposed a mixture of inner-sphere and outer-sphere complexes on HAO at pH 4.5–8.0 based on the XANES data of adsorbed selenite. While our data do not provide any direct indications for the presence of outer-sphere selenite complexes at the γ-Al_2O_3 surface, the possibility of the presence of such complexes in addition to inner-sphere surface complexes cannot be excluded, as the XANES data of our selenite adsorption samples (not shown) are quite similar to those reported by Peak [22]. In addition to outer-sphere complexes, Peak [22] observed the presence of inner-sphere selenite complexes bound in a bridging fashion to the HAO surface, which is the same configuration we observe here for the inner-sphere complexes of selenite coordinated at the γ-Al_2O_3 surface. We conclude that the reactivity of γ-Al_2O_3 toward selenate and selenite is similar to that of HAO, which is consistent with the gibbsite/bayerite $Al(OH)_3$ layer on the γ-Al_2O_3 surface controlling the reactivity of γ-Al_2O_3 toward dissolved species.

5. Conclusions

A combination of macroscopic pH edge experiments, electrophoretic mobility measurements, and X-ray absorption spectroscopic analyses was used to study the interaction of selenate, selenite, and chromate with hydrated γ-Al_2O_3. The pH edge data indicate that adsorption of these oxyanions generally increases with decreasing pH and show that chromate and selenate adsorption is ionic strength-(in)dependent in the pH range 4–9, whereas selenite adsorption is ionic strength-(in)dependent. The adsorption of chromate adsorption peaks at pH 5.0, whereas for selenate and selenite no pH adsorption maxima are observed. Results from the elecotrophoretic mobility measurements show that all three oxyanions contribute negative charge to the surface region bound by the shear plane; however, only selenite decreased the pH_{PZC} of the γ-Al_2O_3 sorbent. The EXAFS data results indicate that selenite ions are coordinated in a bridging bidentate fashion to surface AlO_6 octahedra, whereas no second-neighbor Al scattering was observed for adsorbed selenate ions. Combined, the results presented here show that pH is a major factor in determining the extent of adsorption of selenate, selenite, and chromate on hydrated γ-Al_2O_3. The results point to substantial differences between these anions as to the mode of adsorption at the hydrated γ-Al_2O_3 surface, with selenate adsorbing as nonprotonated outer-sphere complexes, chromate forming a mixture of monoprotonated and nonprotonated outer-sphere adsorption complexes, and selenite coordinating as inner-sphere surface complexes in bridging configuration.

References

[1] D.L. Sparks, in: V. Grassian (Ed.), Taylor and Francis Books Inc., Boca Raton, FL, 2005, p. 3.
[2] G.E. Brown Jr., N.C. Sturchio, in: P.A. Fenter, M.L. Rivers, N.C. Sturchio, S.R. Sutton (Eds.), Mineralogical Society of America, Washington, DC, 2002, p. 1.
[3] E.J. Elzinga, D.L. Sparks, Environ. Sci. Technol. 36 (2002) 1460.
[4] D.G. Strawn, D.L. Sparks, J. Colloid Interface Sci. 216 (1999) 257.
[5] D. Peak, R.G. Ford, D.L. Sparks, J. Colloid Interface Sci. 218 (1999) 289.
[6] A.A. Rouff, E.J. Elzinga, N.S. Fisher, R.J. Reeder, Environ. Sci. Technol. 40 (2006) 1792.
[7] A. Manceau, M. Lanson, N. Geoffroy, Geochim. Cosmochim. Acta 71 (2007) 95.
[8] Y. Arai, E.J. Elzinga, D.L. Sparks, J. Colloid Interface Sci. 235 (2001) 80.
[9] D.G. Strawn, A.M. Scheidegger, D.L. Sparks, Environ. Sci. Technol. 32 (1998) 2596.
[10] S.N. Towle, J.R. Bargar, G.E. Brown, G.A. Parks, J. Colloid Interface Sci. 187 (1997) 62.
[11] A.M. Scheidegger, G.M. Lamble, D.L. Sparks, J. Colloid Interface Sci. 186 (1997) 118.
[12] A. Froideval, M.D. Nero, C. Gaillard, R. Barillon, I. Rossini, J.L. Hazemann, Geochim. Cosmochim. Acta 70 (2006) 5270.
[13] Y. Tang, R.J. Reeder, Geochim. Cosmochim. Acta 73 (2009) 2727.
[14] E.R. Sylwester, E.A. Hudson, P.G. Allen, Geochim. Cosmochim. Acta 64 (2000) 2431.
[15] Z.J. Guo, X.M. Yu, F.H. Guo, Z.Y. Tao, J. Colloid Interface. Sci. 288 (2005) 14.
[16] H. Wijnja, C.P. Schulthess, Soil Sci. Soc. Am. J. 64 (2000) 898.
[17] J.J. Dynes, P.M. Huang, Soil Sci. Soc. Am. J. 61 (1997) 772.
[18] A. Violante, C. Colombo, A. Buondonno, Soil Sci. Soc. Am. J. 55 (1991) 65.
[19] S. Goldberg, C.T. Johnston, J. Colloid Interface Sci. 234 (2001) 204.
[20] H. Wijnja, C.P. Schulthess, J. Colloid Interface Sci. 229 (2000) 286.
[21] J.G. Catalano, C. Park, P. Fenter, Z. Zhang, Geochim. Cosmochim. Acta 72 (2008) 1986.
[22] D. Peak, J. Colloid Interface Sci. 303 (2006) 337.
[23] D. Peak, U.K. Saha, P.M. Huang, Soil Sci. Soc. Am. J. 70 (2006) 192.
[24] D.L. Sparks, Academic Press Inc., San Diego, 2003.
[25] M. Kosmulski, J. Colloid Interface Sci. 298 (2006) 730.
[26] C. Papelis, G.E. Brown Jr., G.A. Parks, J.O. Leckie, Langmuir 11 (1995) 2041.
[27] E.J. Boyle-Wight, L.E. Katz, K.F. Hayes, Environ. Sci. Technol. 36 (2002) 1219.
[28] E.J. Boyle-Wight, L.E. Katz, K.F. Hayes, Environ. Sci. Technol. 36 (2002) 1212.
[29] J.P. Fitts, G.E. Brown Jr., G.A. Parks, Environ. Sci. Technol. 34 (2000) 5122.
[30] Y. Tang, E.J. Elzinga, R.J. Reeder, Geochim. Cosmochim. Acta 71 (2007) 1480.
[31] K.F. Hayes, A.L. Roe, G.E. Brown, K.O. Hodgen, J.O. Leckie, G.A. Parks, Science 238 (1987) 783.
[32] D. Peak, D.L. Sparks, Environ. Sci. Technol. 36 (2002) 1460.
[33] S.E. Fendorf, M.J. Eick, P. Grossl, D.L. Sparks, Environ. Sci. Technol. 31 (1997) 315.
[34] A. van Geen, A.P. Robertson, J.O. Leckie, Geochim. Cosmochim. Acta 58 (1994) 2073.
[35] J.M. Zachara, D.C. Girvin, R.L. Schmidt, C.T. Resch, Environ. Sci. Technol. 21 (1987) 589.
[36] A. Manceau, L. Charlet, J. Colloid Interface Sci. 168 (1994) 87.
[37] H. Wijnja, C.P. Schulthess, Spectrochim. Acta, Part A 55 (1999) 861.
[38] X. Carrier, E. Marceau, J.F. Lambert, M. Che, J. Colloid Interface Sci. 308 (2007) 429.
[39] T. Ressler, J. Phys. IV 7 (1997) 269.
[40] A.L. Ankudinov, J.J. Rehr, Phys. Rev. B 56 (1997) R1712.
[41] K.F. Hayes, J.O. Leckie, J. Colloid Interface Sci. 115 (1987) 564.
[42] R.J. Hunter, in: R.H. Ottewill, R.L. Lowell (Eds.), Academic Press, San Diego, 1981, p. 219.
[43] K. Saeki, S. Matsumoto, R. Tatsukara, Soil Sci. 160 (1995) 265.
[44] A.L. Foster, G.E. Brown Jr., G.A. Parks, Geochim. Cosmochim. Acta 67 (2003) 1937.
[45] J.R. Bargar, G.E. Brown Jr., G.A. Parks, Geochim. Cosmochim. Acta 61 (1997) 2617.
[46] P.C. Hiemenz, R. Rajagopalan, Dekker Inc., New York, 1997.
[47] W. Stumm, J.J. Morgan, Wiley, New York, 1996.